EGG-M-88438

CONF-881011--42

COMPARISON OF THERMAL AND MECHANICAL RESPONSES OF THE TMI-2 REACTOR VESSEL[1]

G. L. Thinnes

Idaho National Engineering Laboratory

EG&G Idaho, Inc.

P.O. Box 1625

Idaho Falls, ID 83415-3503

EGG-M--88438

DE90 002032

Abstract

The TMI-2 accident resulted in approximately 40% of the reactor's core melting and collecting on the lower head of the reactor pressure vessel. The severity of the accident has raised questions about the margin of safety against rupture of the lower head in this accident since all evidence seems to indicate no major breach of the vessel occurred. Scoping heat transfer analyses of the relocated core debris and lower head have been made based upon assumed core melting scenarios and core material debris formations while in contact with the lower head.

---

[1]Work supported by the U.S. Department of Energy, Assistant Secretary for Nuclear Energy, Office of LWR Safety and Technology under DOE Contract No. DE-AC07-76ID01570.

This paper describes the structural finite element creep rupture analysis of the lower head using a temperature transient judged most likely to challenge the structural capacity of the vessel. This evaluation of vessel response to this transient has provided insight into the creep mechanisms of the vessel wall, a realistic mode of failure, and a means by which margin to failure can be evaluated once examination provides estimated maximum wall temperatures. Suggestions for more extensive research in this area are also provided.

INTRODUCTION

The TMI-2 accident resulted in extensive core damage. The defueling effort of the reactor vessel by EG&G Idaho has shown that about 40% of the original core achieved melting temperatures and approximately 20 metric tons of molten core material relocated from the core region and settled on the lower head of the reactor pressure vessel (RPV)[1]. The high temperatures in the RPV wall resulting from this relocation have caused questions to be raised about the margin of safety between the actual accident conditions and those required to breach the vessel.

The usage of simplified methodology for answering these questions is preferable since the information needed to calculate structural capacity of the vessel is not now, nor may ever be, well defined for TMI-2. However, simplification of a complex structural response requires assumptions and approximations which must be verified in order to provide a reasonable estimate of margin-to-failure for vessel rupture. The

objectives of this investigation were to establish a method by which safety margin could be assessed, perform scoping calculations to provide insight into the mechanisms of failure and parameters critical to their cause, and provide some assessment of the validity of using simplified techniques for predicting safety margin of reactor vessels in such severe accidents.

Since the exact scenario of core relocation is not known, bounding assumptions were made in the finite element heat transfer analyses modeling the energy transfer from the molten debris to the vessel wall. The results of these bounding analyses were temperature distributions which could result from the various debris configurations and cooling assumptions. Some of these distributions were identified by simple structural analyses as being able to fail the vessel. The remaining ones required a more detailed evaluation for margin-to-failure determination.

Subsequently, a structural finite element stress analysis[2] was performed considering: a plausible temperature distribution history, operating system pressure, material temperature-dependent plastic and creep properties, and nonlinear structural response. From this analysis, insight is offered upon the possible failure mechanisms and the appropriateness of simplifying assumptions for margin-to-failure determination. Additionally, areas of needed research for improved margin estimates are discussed.

DESCRIPTION OF THE VESSEL LOWER HEAD

The TMI-2 RPV is a skirt supported vessel designed by Babcock and Wilcox. A cross section of the vessel arrangement is shown in Figure 1. The cylindrical portion of the RPV has an inner radius of 217 cm (85.5 in.) and a wall thickness of 24.1 cm (9.5 in.) while the spherical bottom head has an inner radius of 222 cm (87.25 in.) and a minimum wall thickness of 12.7 cm (5.0 in.). The skirt thickness is 5.1 cm (2.0 in.). The vessel has a stainless steel liner of 18-8 weld overlay with a nominal thickness of .48 cm (3/16-in.) and a minimum thickness of .32 cm (1/8-in.). The lower head contains 52 instrument penetration nozzles made of Inconel through which the in-core instrument assemblies access the reactor vessel.

The lower head is constructed of an axisymmetric forged section in the region of the vessel-skirt junction which is indicated in Figure 1. This forging is constructed of SA508-64, Class 2 material. The lower section of the head is constructed of SA533 Grade B, Class 1, plate material. A circumferential full penetration weld connects the forging to the plate section of the head near the shell-skirt junction. For this analysis, the debris was assumed to have settled uniformly on the bottom head. This limits the region of the vessel undergoing thermal attack for an extended period of time to the bottom of the vessel, well away from the full penetration weld but in a region where numerous instrument assembly penetrations are located.

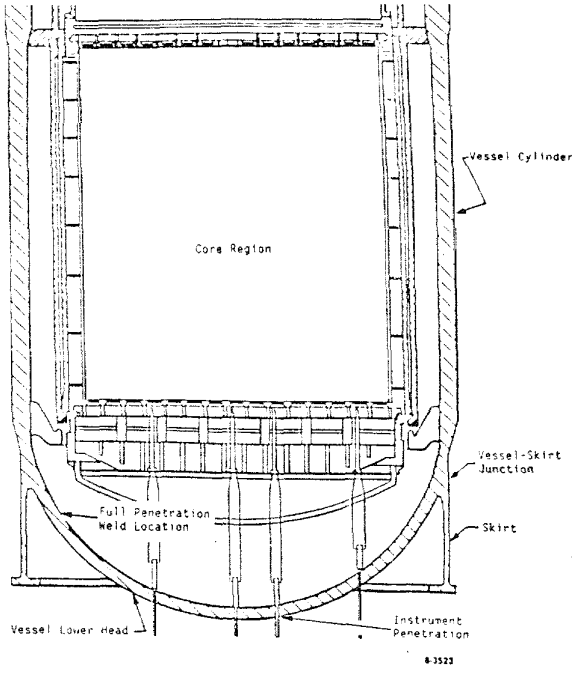

Figure 1. RPV Cross Section

DISCUSSION OF LOWER HEAD MARGIN-TO-FAILURE

Margin-to-failure determination requires knowledge of the vessel head's structural capacity and the loading actually applied to the head. Because of a lack of physical data on the debris bed and no measurements of vessel wall temperatures during the fuel relocation period, the thermal loading on the head was enveloped utilizing limited information known about the debris bed, assumptions in the character of the debris bed, and finite element heat transfer analyses. The mechanical loads were limited to operating system pressure, which was monitored during the relocation. Material properties are not completely defined for temperatures in the upper bound temperature profile. Therefore, estimates in properties were made in the structural finite element models in order to determine vessel capacity.

The following subsections describe the thermal and mechanical loading and discuss the method for making initial estimates of capacity and subsequent selection of temperature profiles for refinement of these estimates by using a structural finite element model.

Bounding Vessel Wall Thermal Histories

A lack of physical data on the lower head debris bed has caused uncertainty in the understanding of the actual rate of heat transfer from the debris to the vessel wall. This affects the wall temperature distribution calculated in the heat transfer analysis and its subsequent effect upon the vessel head's structural analysis. Therefore, a study aimed at bounding the possible vessel thermal response has postulated three debris bed configurations as shown in Figure 2. This study was based upon information from the preliminary inspection of the debris bed.

Figure 2(a) illustrates the debris bed configuration thought to result in an upper bound thermal load in the vessel wall. This consists of a porous debris bed with regions adjacent to the vessel wall having interstices filled with molten control rod material, resulting in a consolidated metallic/ceramic sublayer. This sublayer is assumed to transmit heat to the vessel wall very rapidly. The lower bound case shown in Figure 2(b) is assumed to consist of a layer of solidified control rod material adjacent to the vessel wall which had relocated prior to the major core relocation. This layer was then covered with porous debris from the core. In this case, the layer of solidified control rod material

acts as a heat sink and additional thermal resistance to heat transfer between the debris and the vessel wall.

The cooling of the debris and transfer of heat to the lower plenum coolant is another important uncertainty. Debris cooling was estimated in the calculations by bounding assumptions on the heat transfer and quenching rates of the debris. An upper bound on the rate of debris cooling was assumed to result from water penetration into the debris bed and resulted in cooling of the debris within 20 minutes. A lower bound assumption on the rate of debris cooling assumed no water penetration into the debris bed, thus limiting heat transfer from the debris to: conduction through the debris, surface convection to the coolant at the upper debris surface, and convection and conduction to the vessel wall at the debris/vessel interface.

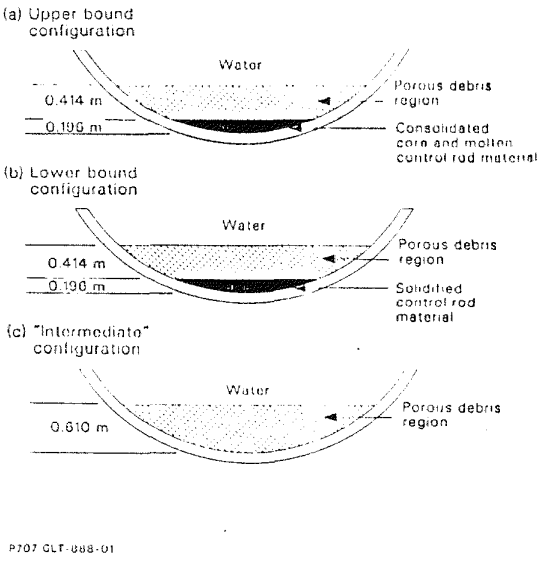

Figure 2. Bounding Debris Configurations

Figure 3 illustrates the results of the heat transfer analyses. The inside vessel wall temperatures, labeled "I.S.", and outside wall temperatures, "O.S.", are indicated. The vessel wall temperatures for the assumption of no liquid penetration and quenching of the porous debris, are shown as solid lines while the temperatures assuming quenching of the porous debris are denoted by dashed lines.

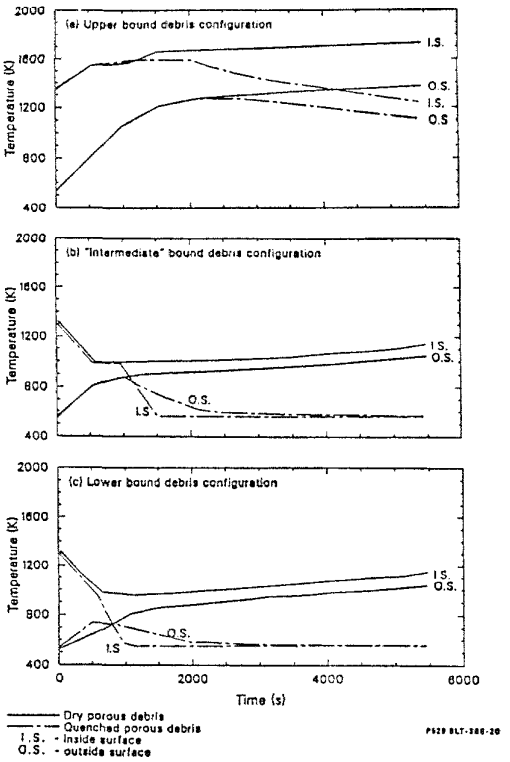

Figure 3. Calculated Temperature Gradients for Bounding Debris Configurations

Mechanical Loads

Figure 4 shows the variation in the operating system pressure during and after the relocation. This pressure, which was monitored by pressure transducers during the accident, was the major contributor to the

mechanical loads on the lower head. The combined pressure on the lower head resulting from water in the RPV and the weight of the core material distributed over the lower head amounted to about .07-.14 MPa (10-20 psi) compared to operating system pressures as high as 11 MPa (1600 psi) during the relocation period. The weight of the reactor vessel is transferred through the cylindrical portion of the RPV down to the skirt support which is well away from the high temperature region. Therefore, the system transient pressure was the only significant force causing primary stress in the lower head.

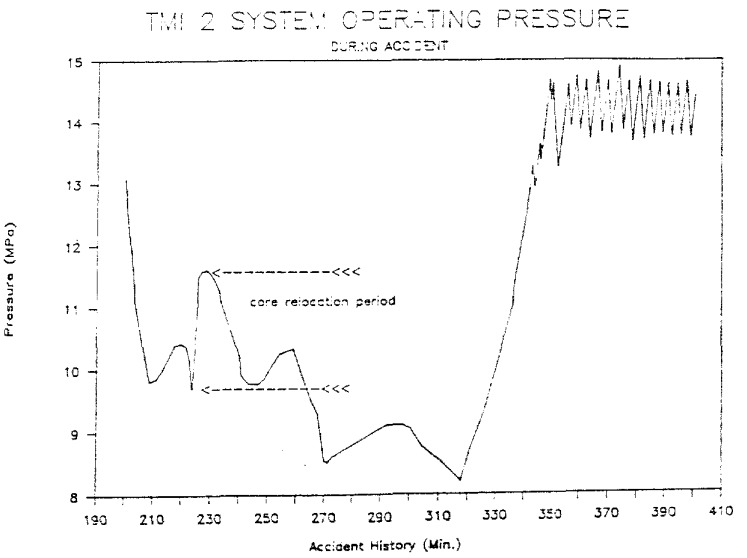

Figure 4. Measured TMI-2 Reactor System Pressure During the Core Relocation and Associated Thermal Transient

This type of stress is not self-limiting, i.e., it does not reach a limit as strains increase. Therefore, this load must always be carried by the lower head vessel wall to maintain structural integrity of the RPV. A simple calculation of the tangential stress in the lower head, a uniform stress through the wall resulting from the system pressure, indicates a

minimum stress resulting from system pressure during the transient of 74 MPa (11 ksi).

Vessel Margin-to-Failure

The effects of creep on a structure's capacity are quite complex and not easily determined when temperatures are not uniformly distributed throughout the structure. This structural characteristic accompanies the material's ultimate strength at temperatures above 700°F for carbon steels such as is found in RPV's. However, since ultimate strength is a temperature-dependent but not a time-dependent material characteristic as is creep, it can be used to screen some temperature distributions out of the list of possibilities, considering that the vessel capacity was not exceeded during the accident.

Inspection of Figures 3(a), 3(b), and 3(c) shows the dry cooling assumption in each debris configuration causes temperature distributions through the wall whose average temperatures trend linearly upward beyond 2000 s after the core relocation. If one extends the ultimate strength curve of SA533 Grade B Class 1, the material in the vessel wall under the settled debris, the ultimate strength is approximately 69 MPa (10 ksi)[2] at 1144K. This is about the minimum stress induced in the vessel wall by operating pressure during the early stages of the relocation when the vessel wall temperatures would be highest. As can be seen in Figure 3, the temperature distributions resulting from the dry debris cooling for all of the configurations either exceed this temperature throughout the wall within the first 2000 s of the transient,

as in the case of the upper bound, or indicates a trend in which minimum wall temperatures would exceed 1144K within 7000 s of the transient in the intermediate and lower bound debris configurations. This would indicate that the dry porous debris cooling assumptions do not appear to be credible without a vessel breach, which does not appear to have happened. By the same reasoning, the upper bound configuration with quenched porous debris cooling would also have low probability of occurrence.

This essentially leaves the intermediate and lower bound configurations with the quenched porous debris cooling assumption being the more probable temperature scenarios. In both cases, the inside temperature would be temporarily high enough to reduce the ultimate strength on the inside below expected pressure stresses; however, the outside temperatures would be low enough that ultimate strength could easily exceed expected primary stresses. Therefore, these scenarios could not be screened out for having low probability of occurrence in the simplistic manner discussed above. Thus, these scenarios were ones requiring closer scrutiny with a detailed structural model.

MODELING OF THE DEBRIS HEAT TRANSFER AND THE VESSEL WALL STRUCTURAL RESPONSE

The screening process was performed to focus on the more probable temperature histories in the accident. The gross assumption of neglecting the effects of thermal bending in the wall did not allow a determination

with high certainty of the possible failure modes of the accident. It only produced a place to start the analysis. By use of the detailed stress analysis, insight into the effects of thermal bending, creep, and plasticity was anticipated.

The intermediate level debris configuration was chosen as the transient to investigate since it was the more stringent of the two remaining plausible transients when vessel creep response was considered.

Heat Transfer Model

Figure 5 shows a schematic of the axisymmetric finite element heat transfer model of the lower head and relocated core material. The illustration indicates locations, or stations, along a meridian of the lower head for which radial temperature distributions are defined for the structural model of the lower head. This particular model is a modification of the original model by Moore[1] using the COUPLE/FLUID[3] finite element code to provide a radial temperature distribution at five points through the wall corresponding to nodal locations on the structural model. This heat transfer code solves the two dimensional energy transport equation using quadratic elements.

The heat transfer model of the debris and lower head of the vessel assumes axisymmetric behavior around the RPV centerline and consists of a porous debris region of 121 elements and a vessel wall region of 44 elements. The outer surface of the vessel wall simulated heat transfer

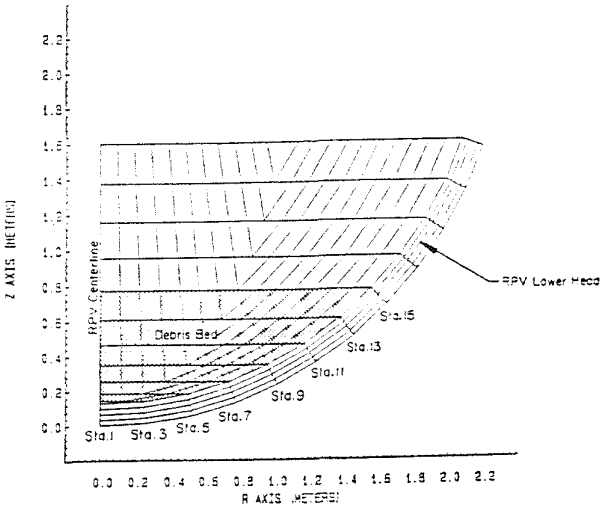

Figure 5. COUPLE Finite Element Model of TMI-2 Lower Head Debris and Vessel Wall

through the thermal shield to the interior of the RPV support pedestal. The containment temperature was assumed to be 311K (100°F) and the initial temperature of the head was 559K (547°F) while the initial debris temperature was assumed to be 2500 K (4040°F). A quench time of 20 min was used and the quench front was assumed to move radially from the outer edge of the debris bed towards the vessel centerline. A constant energy removal rate from the debris was assumed to determine the radial quench front location with respect to time for the analysis.

Figures 6 through 11 plot the temperature histories at the five radial points through the wall at stations 1, 2, 3, 13, 14, and 15 with inner surface temperatures being initially hottest. These temperature histories correspond to the analysis of the intermediate level debris configuration with quenched cooling. The quench front, i.e., the cooling wave moving

from the edge of the debris to the centerline of the vessel, is represented in Figures 6 through 11 by the abrupt drop in inner surface temperature. The first three stations (indicated on Figure 5) range from the RPV centerline outward while the last three stations show temperature distributions near the outer edge of the relocated debris. Stations 4 through 12 are not plotted but offer intermediate values in temperatures and quench front times. The rest of the structure was assumed to remain at a constant temperature of 559K throughout the structural analysis.

Structural Model

An axisymmetric model of the lower head, skirt, and a cylindrical portion of the RPV was made using the ABAQUS[4] nonlinear structural finite element code. An eight node, axisymmetric continuum element, the ABAQUS CAX8 element, was the primary element used in the model. This element uses a biquadratic interpolation with 3 x 3 integration. The model is shown in Figure 12. The critical portion of the model, the spherical head region below the skirt junction, was modeled with two elements through the thickness and ten along the meridian of the lower head up to the skirt junction. Symmetrical boundary conditions were applied at the RPV centerline degrees of freedom while boundary conditions of continuity at the degrees of freedom on the cylindrical portion of the RPV axisymmetric model were imposed.

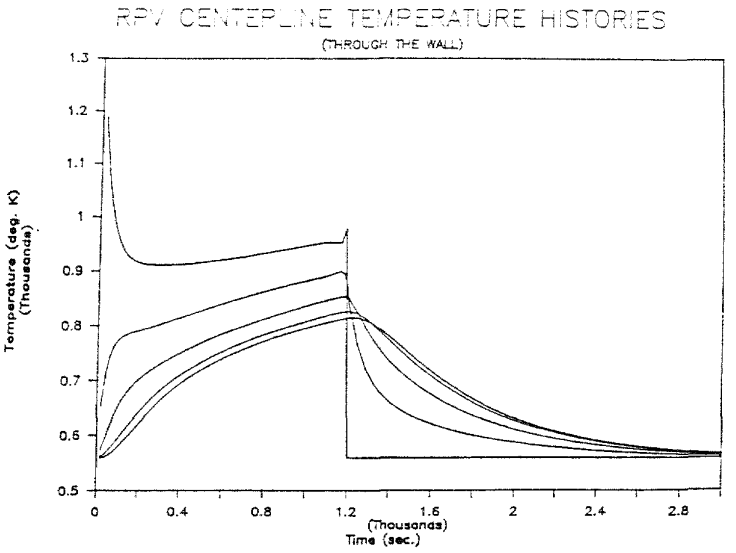

Figure 6. RPV Centerline Temperature Histories

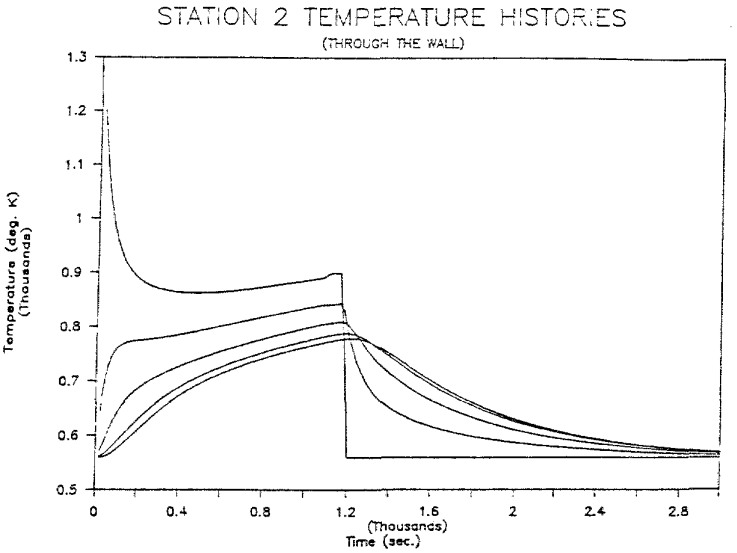

Figure 7. Station 2 Temperature Histories

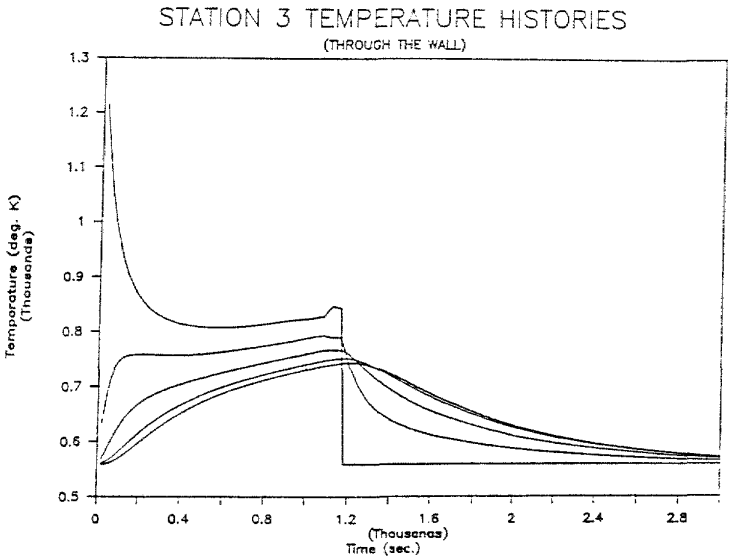

Figure 8. Station 3 Temperature Histories

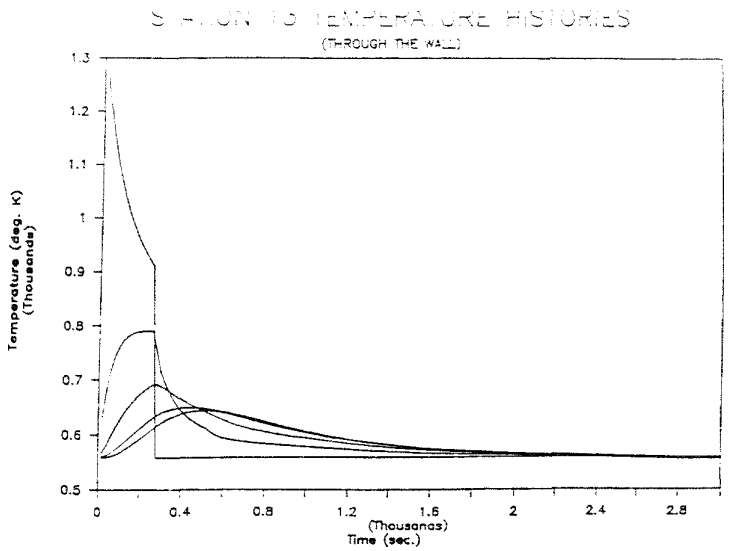

Figure 9. Station 13 Temperature Histories

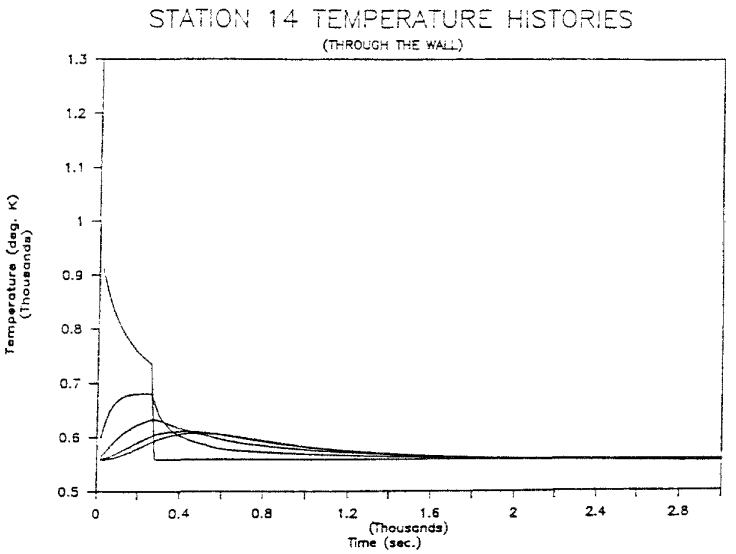

Figure 10. Station 14 Temperature Histories

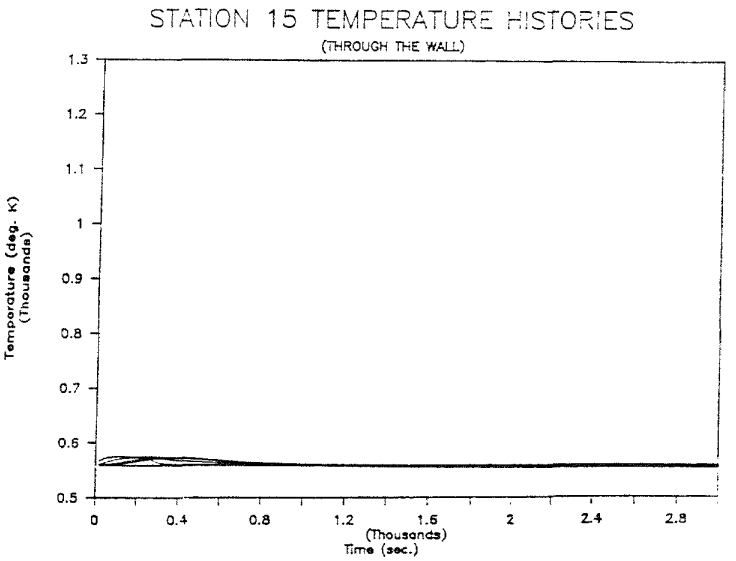

Figure 11. Station 15 Temperature Histories

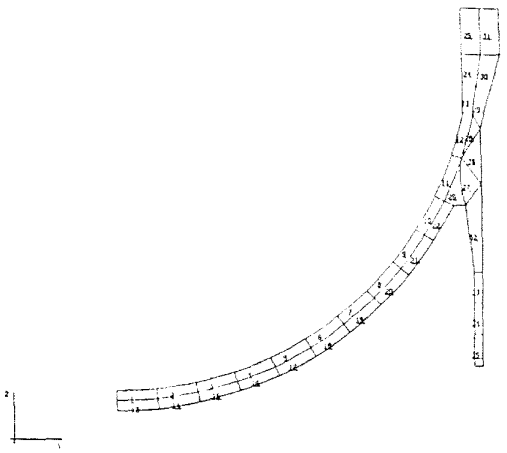

Figure 12. TMI-2 Lower Head Structural Model

Since the scope of this analysis was limited to an axisymmetric response of the lower head to the core relocation, the plate material, SA533, Grade B Class 1, was the primary material of concern. Some creep rupture data for this material have been reported by Smith.[5] High-temperature elastic-plastic and creep properties for SA533 Grade B, Class 1 material have been documented by Reddy and Ayres[6] from tests performed up to 922K (1200°F). Such properties beyond this temperature are not available at this time. The ABAQUS model uses the 922K properties for any higher temperatures encountered at the element integration points.

The creep strain plots from Reference 6 compare test data with an analytical constitutive equation developed to represent that test data. That equation relates creep strain to temperature, effective stress, and time in the following general form:

(1) $$\epsilon_c = A^B \left(\frac{\sigma}{\sigma_m}\right)^C t^B$$

where: ϵ_c = creep strain

A, B, and C = functions of temperature

t = creep time

σ = effective stress

σ_m = function of effective stress and temperature.

Inspection of these comparison plots show that the actual test data for the higher temperatures was limited to smaller stress ranges. As will be discussed later in more detail, some effective stresses encountered in the TMI-2 analysis were beyond these stress ranges and the constitutive law was used as an extrapolation to this test data to approximate creep strains at the higher stresses.

The temperature dependent stress-strain curves of Reference 6 were used in the structural model's material properties. The Reference's temperature dependent mean coefficients of thermal expansion, Young's moduli, and yield stresses were also utilized in the model and documented in Reference 2.

Time varying temperatures were applied at all nodes in the vessel wall in the debris region of the structural model. The remainder of the model nodes were kept at a constant 560K (547°F).

Since isoparametric finite elements were used in this analysis, elemental properties are determined as a function of element integration point temperatures. These temperatures are determined via an interpolation, or shape, function which is dependent upon the chosen element type. A quadratic polynomial is used to interpolate nodal temperatures of each element to get integration point temperatures. This interpolation causes a significant difference between the inner wall nodal temperatures and the inner most integration point temperatures in the structural elements. This seems justifiable since, for the given temperature scenario, the extreme temperatures are highly localized in the region of the inner surface of the vessel wall. Thus, the affected region would load up, stress relieve, and redistribute load on the inner elements in a smoothing manner similar to the effect of interpolation. This is an approximation which seems appropriate since increased accuracy of the temperature representation at the elemental level would require a very large increase in model size. As a result of this temperature interpolation, maximum integration point temperatures encountered in the structural model were approximately 1000K (1340°F) which is only slightly higher than temperatures for which material creep and ultimate strength test data are available.

In addition to the temperature loading, the reactor system operating pressure time history of Figure 4 was applied at all elements on the inside surface of the structural model. This pressure ranged from a maximum of 11.6 mPa (1683 psi) to a minimum of 9.7 mPa (1406 psi) during the analysis.

The structural analysis was broken into three sequential steps. The first step brought the structure to a static equilibrium state at 9.7 MPa (1407 psi) internal pressure and a uniform temperature of 559K (547°F). There was no nonlinear structural behavior during this step. These were the conditions prior to the relocation transient. This condition produced an average effective stress (von Mises stress) in the wall of 86.9 MPa (12.6 ksi) which agreed with the calculation:

$$(2) \qquad \sigma = \frac{pr}{2t}$$

where: σ = tangential stress in a sphere

p = internal pressure

r = mean radius of the sphere

t = wall thickness

This stress changed very little throughout the region of the model under the debris indicating very little influence resulting from boundary effects in this critical region for uniform pressure loading.

The second step of the analysis kept the internal pressure loading at a constant 9.7 MPa but increased nodal temperatures in the vessel wall under the debris to the initial values of the temperature transient which is partially illustrated in Figures 6 to 11. The structural model incurred plastic deformation but had no material (time-dependent) creep properties in this step.

The third and final step utilized the end state of the second step for initial conditions and added material creep properties to the structural model. This third step analyzed the time-dependent nonlinear structural response of the lower head to the internal pressure loading exhibited in Figure 4 and the nodal temperature histories exemplified in Figures 6 to 11. This analytical step extended over the first 1600 s of the loading transients.

RESULTS

Figures 13 through 16 illustrate 16 discrete views, in time, of the temperature transient at the element integration points and resulting stress distribution in the axisymmetric structural analysis of the TMI-2 lower head after core relocation. Contour lines connect regions of equal temperature in the four plots on the left side of each figure while on the right side they connect regions of equal stress. The time, in seconds, after initiation of the thermal transient at which these stresses were calculated, is indicated in the center of each figure. The stress component illustrated is orientated parallel to the "1" axis indicated in the lower left corner of each figure. This component of stress was selected because it was typically larger than the hoop direction component and offers the clearest picture of the stress scenario resulting from this postulated thermal transient. The four figures cover a period of about 1600 seconds after core relocation.

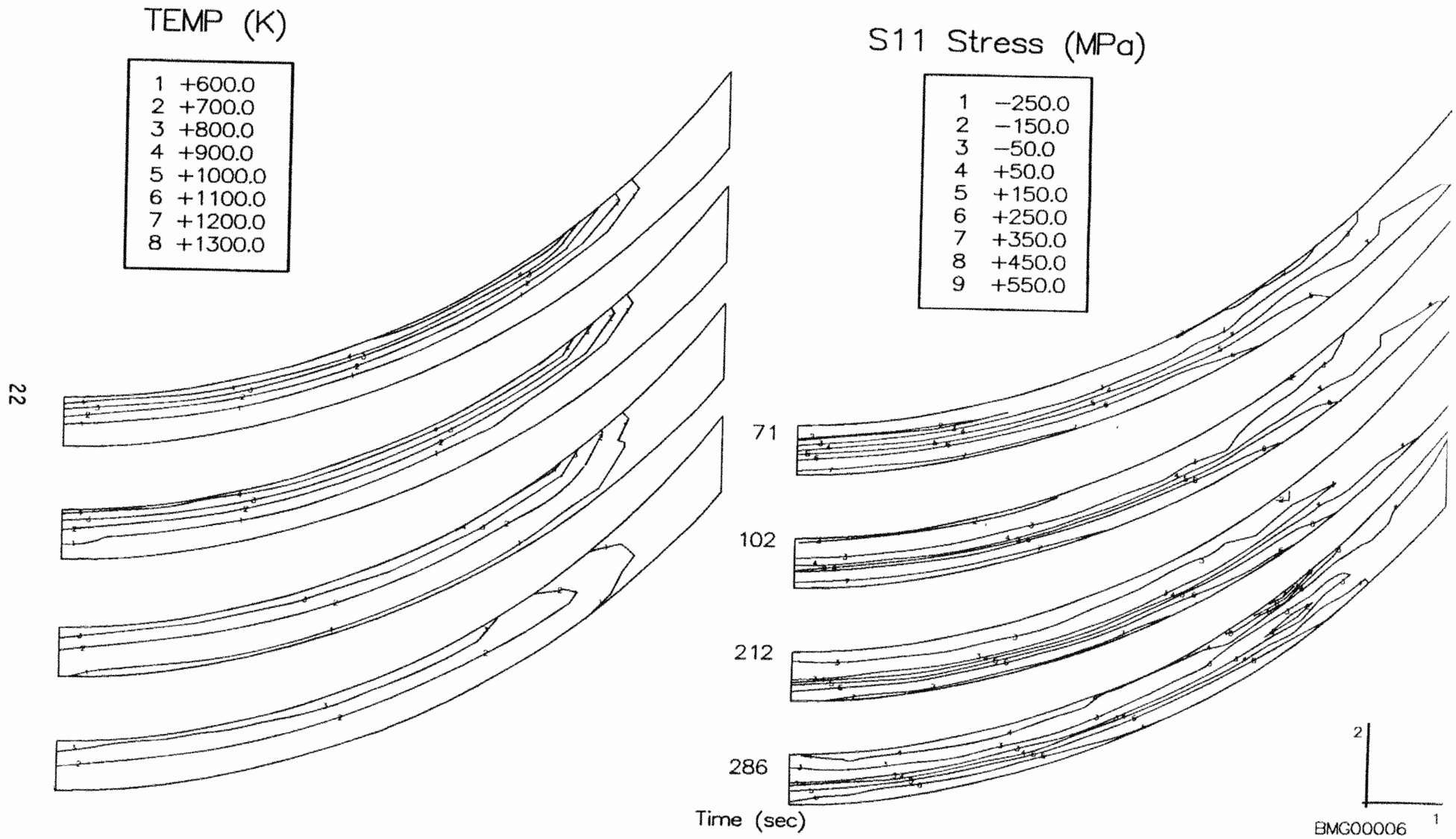

Figure 13. RPV Wall Temperature and Stress Distributions

(Thermal Transient Period Through 286 Seconds)

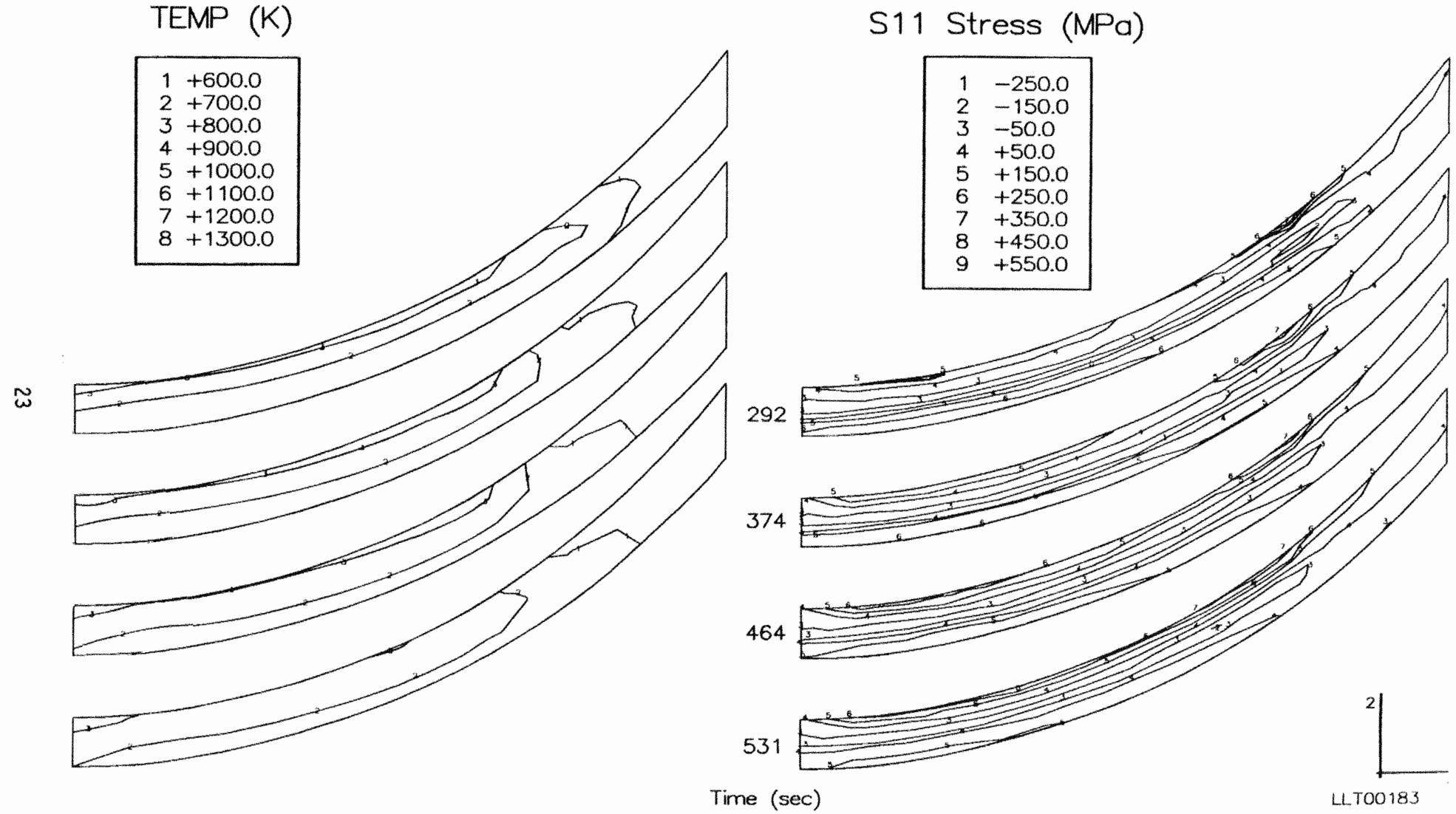

Figure 14. RPV Wall Temperature and Stress Distributions

(Thermal Transient Period 292 Through 531 Seconds)

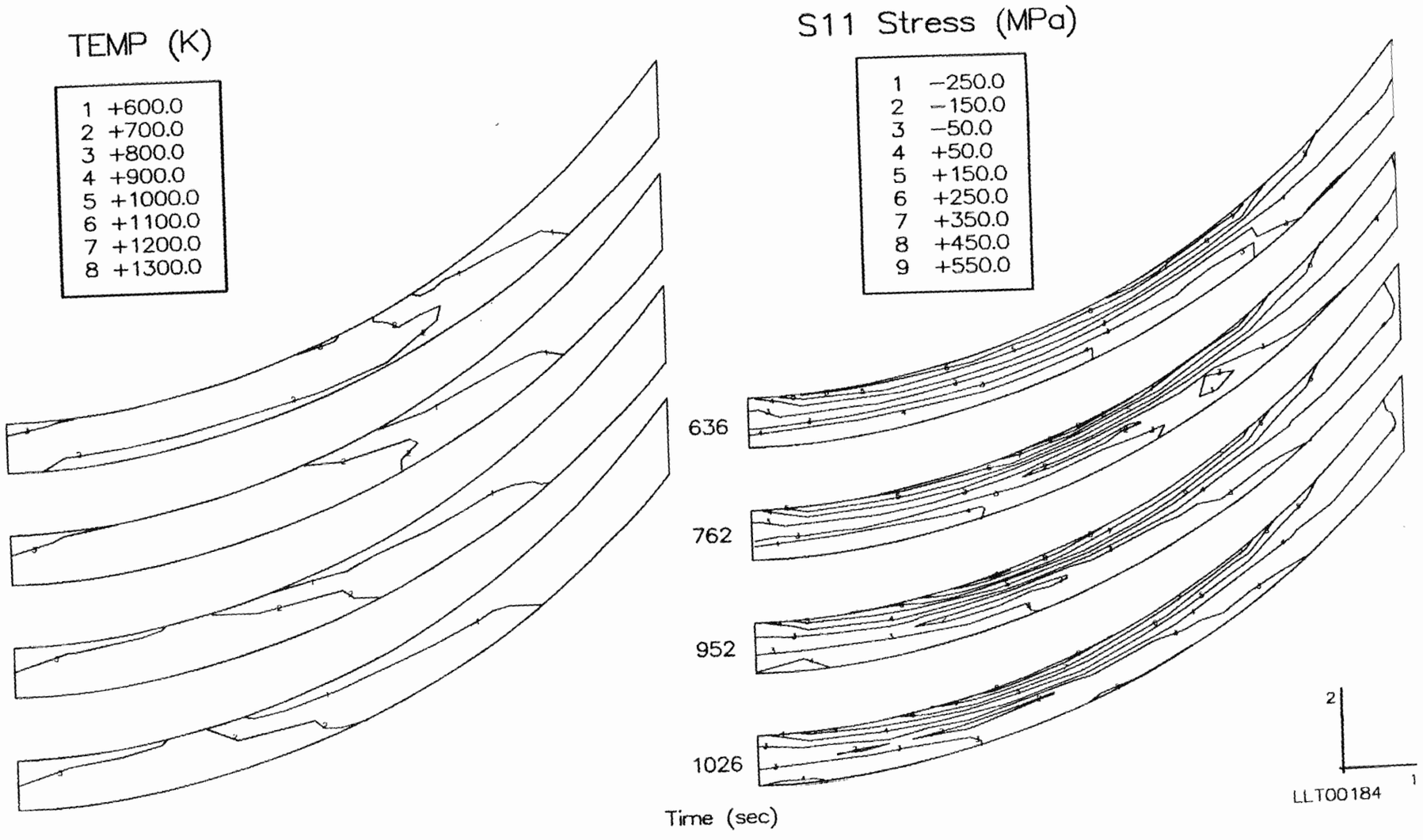

Figure 15. RPV Wall Temperature and Stress Distributions

(Thermal Transient Period 636 Through 1026 seconds)

Vessel Inelastic Response
Transient Period 1056 thru 1601 seconds

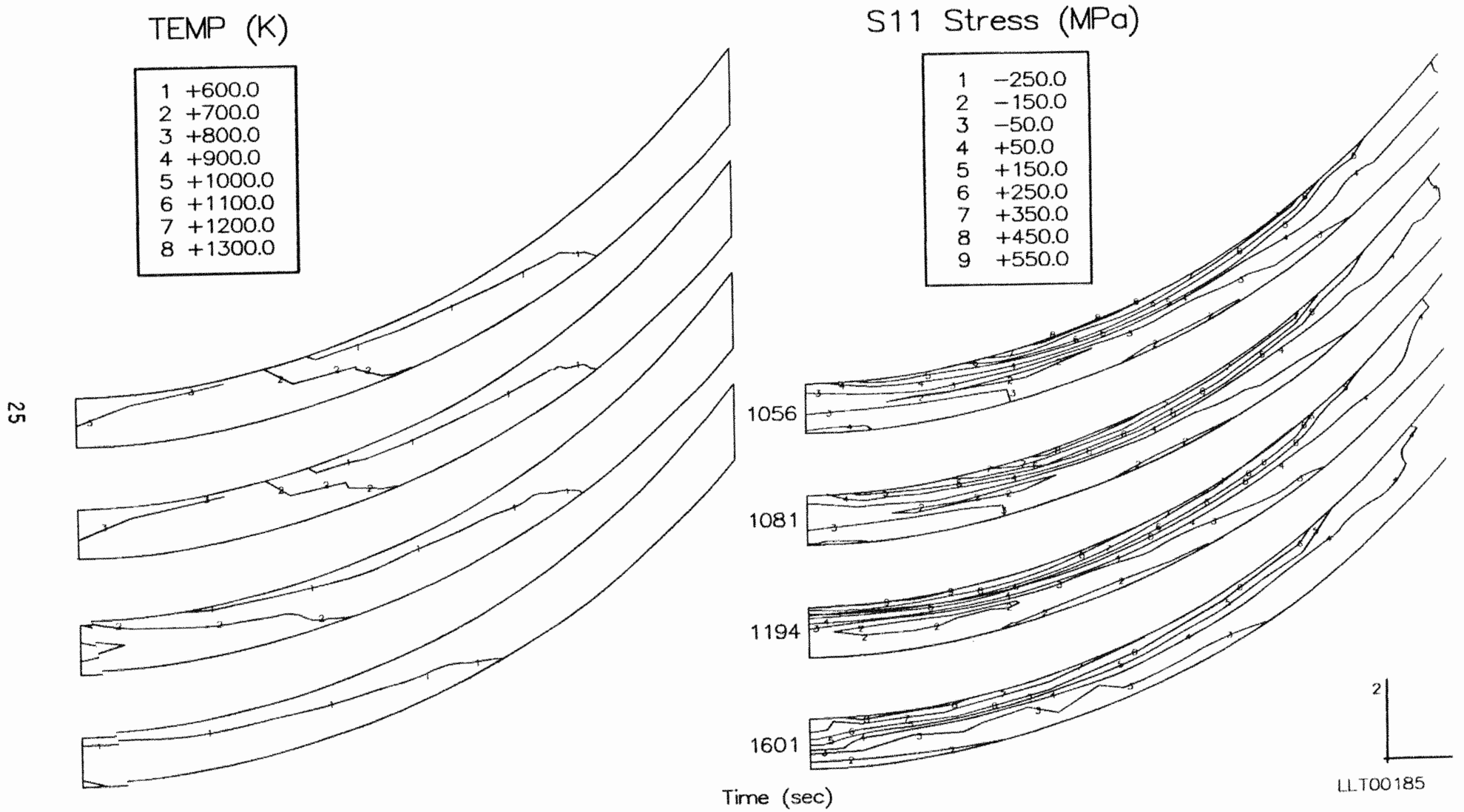

Figure 16. RPV Wall Temperature and Stress Distributions

(Thermal Transient Period 1056 Through 1601 Seconds)

As indicated in Figure 13, the unquenched temperature gradient is maintained in the vessel wall until about a time of 212 seconds. The high initial gradient reduces in time because of the exponential reduction of the inner wall surface temperature over this part of the transient as seen in Figures 6 through 11. During this period, stress distribution through the wall consists of compression on the inside and tension on the outside as the hotter inner portion expands and is constrained by the colder outer portion. This is, essentially, a bending stress distribution through the wall during this interval. Note the high stress gradient at the midsurface which indicates high shear stresses in the midsurface region as well as high meridional stresses on the inner and outer portions of the vessel wall. Material yielding occurs in both the inner and outer portions of the vessel wall during this interval.

Approximately 282 seconds into the transient the quench starts as indicated by the temperature contours "curling back" toward the RPV centerline near the inner surface at the outer edge of the debris bed. This is in response to the cooling inner wall temperatures. This produces a localized tension-compression-tension stress gradient through the wall at the quench front. This gradient attenuates spacially towards the RPV centerline from the current quench front location but maintains its basic configuration.

In the succeeding time frames, the temperature contours migrate towards the RPV centerline as the quench front progresses towards the

center of the debris bed. A high local stress gradient through the wall continues to accompany the quench front as it moves. Trailing the quench front, the localized tension-compression-tension distribution gives way to a residual bending stress which has reversed direction from the pre-quench distribution. At 1601 seconds, the temperature gradient is much more uniform and lower than the initial phases signaling the end of significant thermal effects on the vessel wall.

Throughout the thermal transient, note that the highest stress gradients generally occur on the inner half of the vessel wall. This might offer a signature for this postulated temperature scenario which could be identified in post-accident examination.

Even though yielding did occur at various times at locations distributed throughout the wall thickness, the inelastic deformations were rather small. Maximum elastic strains, including thermal expansion, were of the order of 2% while maximum plastic and creep strains were each approximately 1%.

From this picture of the structural response to the given temperature history, a list of critical parameters to the severity of stress in the wall can be made. They are as follows:

1. Thermal conductivity through the vessel wall
2. Heat capacity of the material
3. Quench front velocity
4. Contact temperatures

5. Creep and plasticity properties of the wall material above 922K (1200°F)
6. Creep properties in the 672K (750°F) to 922K at high stress.

The first four parameters affect the severity of the thermal loading while the last two affect severity of material deformation.

CONCLUSIONS AND RECOMMENDATIONS

The state of stress through the vessel wall for this transient is quite complicated. The overall stress gradients are dominated by the thermal gradients in the vessel wall under the debris bed. Plastic and creep deformations occur causing redistribution of stress throughout the wall thickness. Stress gradients also undergo reversals over the life of the transient. Plastic deformations occur at various locations throughout the wall thickness at various times during the transients. Both compressive and tensile yielding occur on the inner half of the wall while primarily tensile yielding is exhibited in the outer portion. Even though plastic deformation was widely distributed, it was not very high. Maximum plastic and creep strains were each in the 1% range. Reference 5 reports creep rupture strains at 783K (950°F) of about 35% and elongations at ultimate strength and 783K (950°F) of about 25%.

Inelastic material test data for SA533 Grade B Class 1 material are presently only available for temperatures up to 922K. This transient had a brief period in which a highly localized portion of the vessel wall

inner surface experienced temperatures as high as 1255K (1800°F). Because of the elemental shape functions, the highest integration point temperatures were about 1000K (1350°F). It is estimated that inclusion of these properties, if they were known for the higher temperatures, would increase plastic deformations in the majority of the wall only a minimal amount because of the highly localized distribution of these high temperatures.

From these scoping calculations it is concluded that rupture of the lower head resulting from large temperature differences across the vessel wall is not very probable. The temperature distribution used here restricts the high temperatures to the inside surface and the transient is really not long enough to mobilize any significant creep in the wall which would lead to rupture. For this type of temperature distribution, creep only causes the high thermal compressive stresses on the inner surface to relieve rather quickly and cause the wall to carry load in its outer portions.

Because a large thermal gradient across the vessel wall does not appear to cause rupture, the more probable failure mode for rupture would occur at high uniform temperatures in the wall. When a significant portion, such as half of the vessel wall thickness or more, experiences temperatures at which ultimate strength of the head material is approximately 68.95 MPa (10 ksi) and this temperature level occurs over a fairly large area of the lower head, rupture would more likely occur. A more definitive estimate of the required distribution of high temperatures to cause rupture would require further analysis and additional high temperatures testing of the SA533 material.

The part of the lower head which could cause vessel wall rupture and which is more susceptible to creep than the SA533 material is the full penetration weld connecting the forging with the plate material in the head. This is because the welding process reduces ductility and, thus, allowable creep strains in the heat affected zone[7]. However, this weld is higher on the head and, based on this analysis and the postulated length of relocation time, it does not appear that high enough temperatures could be reached through a large enough portion of the wall to cause substantial creep strain in the weld.

Another area of concern for creep rupture is around the lower head penetrations. These penetrations consist of Inconel nozzles with sleeves fitted through holes approximately 2.54 cm (1 in.) in diameter bored in the lower head and welded at the nozzle base to the vessel inner surface. If rupture of the nozzle occurred, molten material could possibly flow down through the penetration until lower temperatures in the penetration walls froze the material in the tube. Again, because of the highly localized temperatures, the effect in penetrations would also seem to be localized but further investigation into the effect on the penetration assembly should be evaluated in more detail.

REFERENCES

1. Tolman, E. L. and Moore, R. A., "Estimated TMI-2 Vessel Thermal Response Based on the Lower Plenum Debris Configuration", Joint AIChE/ASME Heat Transfer Conference, High Melt Attach Phenomena Session, Houston, TX, July 24-27, 1988.

2. Thinnes, G. L., "TMI-2 Lower Head Creep Rupture Analysis", EG&G Idaho Report, EGG-TMI-8133, August 1988.

3. Lemon, E. C., "COUPLE/FLUID, a Two-dimensional Finite Element Thermal Conduction and Convection Code, EG&G Idaho Report,ISD-SCD-80-1, February 1980.

4. "ABAQUS User's Manual (Version 4.6)", Hibbitt, Karlsson & Sorensen, Inc., Providence, Rhode Island, 1987.

5. Smith, G. V., "Evaluations of the Elevated Temperature Tensile and Creep-Rupture Properties of C-M_o, M_n-M_o, and M_n-M_o-N_i Steels", Metal Properties Council, American Society for Testing and Materials, ASTM Data Series Publication DS47, 1971.

6. Reddy, G. B. and Ayers, D. J., "High Temperature Elastic-Plastic and Creep Properties for SA533 Grade B Class 1 and SA508 Materials", Electric Power Research Institute Report No. NP-2763, December 1982.

7. V. N. Shah ltr to C. R. Toole, (EG&G Idaho ltr) VNS-028-85, Severe Accident Extension Project, December 12, 1985.